

into the gas of the positive column. The temperature profile is approximately symmetric (see Fig. 3b) and the thermal fluxes are similar. The later rate of temperature increase in the cathode dark space is determined by the time required for gas heating over the entire discharge interval. The quantity of heat removed by thermal conductivity to the cathode increases and $\delta \rightarrow 1$.

We note that the calculations were performed for a small interelectrode gap with the goal of machine-time economy (one calculation variant required ~ 2 h). This does not decrease the generality of the conclusions reached as to the effect of gas heating on the characteristics of a discharge with arbitrary interelectrode gap. While the discharge burns the gas region near the cathode serves as a perturbation source and the amplitude of the wave changes only slightly. In the calculated intensely anomalous regime the Mach number $M = 2$ ($M = D/c_0$, where D is the shock-wave front velocity), and at $t = 1.5 \mu\text{sec}$, $M = 1.4$. Shock-wave attenuation intensifies with motion through the decaying plasma. The pressure behind the shock-wave front falls off as $z^{-1/2}$.

LITERATURE CITED

1. F. E. Culick, P. I. Shen, and W. S. Griffins, "Acoustic waves and heating due to molecular energy transfer in an electric discharge CO laser," *IEEE J. Quant. Electron.*, 12, 566 (1976).
2. W. M. Clark, "Optic homogeneity of ultraviolet-preionized CO₂-laser discharge," *Appl. Opt.*, 13, No. 9 (1974).
3. A. N. Lobanov, Ya. M. Londer, et al., "Cathode layer dynamics in a dependent glow discharge," *Zh. Tekh. Fiz.*, 52, No. 10 (1982).
4. A. L. Ward, "Calculation of cathode-fall characteristics," *Appl. Phys.*, 9, 2789 (1962).
5. D. H. Pringle and W. E. J. Farvis, "Electron groups in the helium negative glow," *Phys. Rev.*, 96, 536 (1954).
6. V. A. Shveigert and I. V. Shveigert, "The cathode region of a glow discharge in inert gases," in: *High Power CO₂-Lasers for Plasma Experiments and Technology* [in Russian], Novosibirsk (1986).
7. S. Ya. Bronin, V. M. Kolobov, et al., "Normal current density in a dependent glow discharge," *Teplofiz. Vys. Temp.*, 18, No. 1 (1980).
8. V. V. Zakharov, A. A. Karpikov, and E. V. Chekhunov, "Volume gas discharge in nitrogen with steady-state external ionization," *Zh. Tekh. Fiz.*, 46, No. 9 (1976).

EFFECTS OF AEROSOL PARTICLES ON CORONA-DISCHARGE PARAMETERS AND TRANSPORT CURRENT IN A ONE-DIMENSIONAL ELECTROHYDRODYNAMIC FLOW

N. L. Vasil'eva, G. L. Sedova,
and A. V. Filippov

UDC 532.5:537

A unipolar charged aerosol consists of a gas, ions of one sign, and dispersed-phase particles, in which the latter may be charged by the ions [1]. Here we present a theoretical study on this as affecting electrohydrodynamic flows. We have examined continuous stationary one-dimensional flows on the basis of particle electrification between two parallel grids perpendicular to the flow. The electric field and the particles influence the gas motion to a negligible extent. We envisage cases where the first grid is a corona source, while the incident flow contains the particles, and also where the first grid is the particle source and the incident flow contains the positive ions. Such flows are one-dimensional analogs for an aerosol flow around a corona source and flow of a unipolar gas around an aerosol source. We have examined how the particles influence the voltage-current characteristics in the corona and the total current arising from transport of ions and charged aerosol particles between the grids. In both cases, we have calculated the electrification for the aerosol flowing

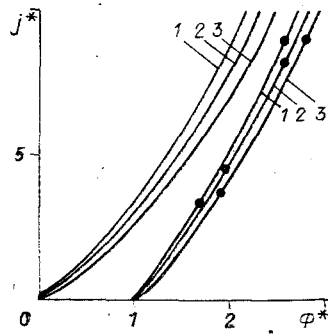


Fig. 1

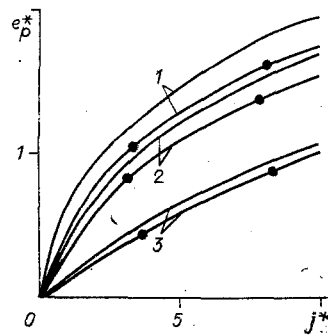


Fig. 2

between the grids correspondingly for a finite surface ion absorption rate on diffusion-limited charge transfer [2] and with allowance for the joint effects of that transfer and charging caused by the field [3]. For some limiting cases, we have obtained asymptotic formulas. Analogous flows have been examined in [4] for a unipolar charged gas. Our results agree with [4] when the particle concentration tends to zero. A study has also been made in [5] on how aerosol particles affect the corona characteristics when the particles are charged along an electric field (i.e., without allowance for ion diffusion).

1. We consider a one-dimensional stationary flow of aerosol consisting of a gas and originally uncharged particles which passes through a region of unipolar corona discharge between two flat grids perpendicular to the flow. For definiteness we assume that the collector electrode is grounded (zero potential), while the emitter electrode has a system of needles producing the corona, which begins at the potential Φ_0 . The distance L between the electrodes is large enough for the field inhomogeneity at the electrodes to be negligible. We take a cartesian coordinate system x, y, z such that emitter and collector lie in the planes $x = 0$ and $x = L$. Without loss of generality, the ions are taken as positive. The parameters characterizing the electrical and inertial forces acting on the particles are taken as small:

$$B \equiv e_p^0 E^0 / (6\pi\mu a |u|) = D / (6\pi\mu b^2) \ll 1, \quad \text{Stk} = mu / (6\pi\mu a L) \ll 1.$$

Here $e_p^0 = aD/b$; $E^0 = u/b$ are the characteristic particle charge and field strength, D and $b \equiv eD/kT$ being the ion diffusion coefficients and mobilities, e the proton charge, k the Boltzmann constant, u and μ the gas flow speed and viscosity, and a and m the particle radius and mass. Then one assumes that the gas and particle speeds are the same and are $u = \text{const}$, while the particle concentration is constant: $n_p = \text{const}$. This flow is a one-dimensional analog for an aerosol flowing around a corona source. The differential equations for the particle charging on passage through the discharge are as follows, together with the field distribution and the charge density between the grids, in addition to the boundary conditions there:

$$u \frac{de_p}{dx} = I, \quad I = 4\pi q a D I^* \left(\frac{abE}{D}, \frac{be_p}{aD}, \frac{be_p}{aK^2} \right); \quad (1.1)$$

$$\frac{dE}{dx} = 4\pi (q + e_p n_p), \quad E = -\frac{d\varphi}{dx}, \quad q(u + bE) + e_p n_p u = j = \text{const}; \quad (1.2)$$

$$\varphi(0) = \Phi, \quad E(0) = \Phi_0/L \equiv E^0, \quad e_p(0) = 0, \quad \varphi(L) = 0, \quad (1.3)$$

in which K is the rate constant for ion attachment to particles, φ potential, Φ emitter potential, $\Phi > \Phi_0$; Φ_0 the corona discharge striking potential, j density of the total current represented by the ions and particles, q the ion charge density, u and E the projections of vectors u and E on the x axis, and I the current flowing to a particle from ions depositing on it. The second boundary condition in (1.3) means that the field strength at the emitter remains unaltered as Φ increases after the corona strikes.

We consider particle charging by diffusion when the condition $Pe_E \equiv ea|E|/kT \ll 1$ is met throughout the flow. For a finite attachment rate to the particles, the electrification current is [2]

$$I^* = \frac{4\pi b q e_p}{[1 + be_p/a^2 K] \exp(be_p/kT) - 1}.$$

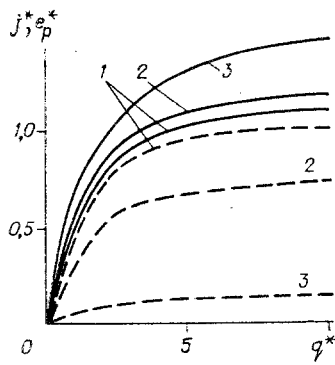


Fig. 3

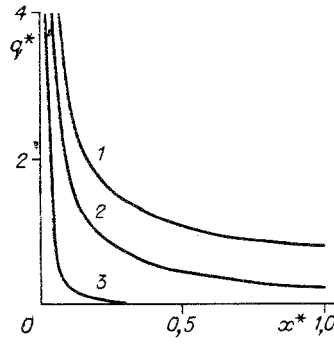


Fig. 4

The conditions $Stk \ll 1$, $B \ll 1$, $Pe_E \ll 1$ are met for an aerosol flow having the characteristic parameters $a \sim 10^{-6}$ m, $u \sim 10$ m/sec, $b \sim 2 \cdot 10^{-4}$ m²/(V·sec), $D \sim 10^{-5}$ m²/sec, $\mu \sim 2 \cdot 10^{-5}$ kg/(m·sec), $L \sim 10^{-1}$ m, $E \sim 1$ kV/m. In [5], the flows had substantially larger a and E , for which $Pe_E \gg 1$, $B \geq 1$.

We convert to the dimensionless variables

$$E^* = \frac{bE}{u}, \quad e_p^* = \frac{be_p}{aD}, \quad q^* = \frac{4\pi bLq}{u}, \quad \varphi^* = \frac{\varphi b}{uL}, \quad j^* = \frac{4\pi b j L}{u^2},$$

$$x^* = \frac{x}{L}, \quad K^* = \frac{Ka}{D}. \quad (1.4)$$

The equations then contain the dimensionless parameter $N \equiv 4\pi a D L n_p / u$, which characterizes the effects for the particles on $E^*(x^*)$, $q^*(x^*)$, $e_p^*(x^*)$.

Equations (1.1) and (1.2) have an integral relating e_p^* to E^* in general form; this takes particularly simple forms for $N \ll 1$ and $N \gg 1$. For $N \ll 1$, we can neglect the terms proportional to the particle concentrations and get from (1.1) and (1.2) that

$$E^* = C + Ei(e_p^*) - \ln e_p^* + \frac{1}{K^*}(\exp e_p^* - 1), \quad (1.5)$$

in which $Ei(e_p^*)$ is the integral exponential function and C a constant defined from (1.3). The $E^*(x^*)$ and $q^*(x^*)$ distributions and $j^*(\varphi)$ are here independent of particle effects [6].

For $N \gg 1$, the maximum charge on a particle is attained when all the ions have deposited on particles and thus $q^* = 0$, where the third equation in (1.2) gives $|e_p^*| < \max |e_p^*| = |j^*/N| \ll 1$. Then (1.1) and (1.2) give a differential equation for $E^*(e_p^*)$, whose general solution is

$$E^* = \left[-A^{1-A} \left(\Gamma \left(A, A \left(1 - \frac{N}{j^*} e_p^* \right) \right) + C_0 \right) \right] \left(1 - \frac{N}{j^*} e_p^* \right)^{-A} \exp \left[A \left(1 - \frac{N}{j^*} e_p^* \right) \right],$$

$$A \equiv \frac{j^*}{NP}, \quad P \equiv \frac{K^*}{1 + K^*}. \quad (1.6)$$

For arbitrary finite N , (1.1)-(1.3) should be solved numerically.

Figures 1 and 2 give numerical results. Figure 1 shows the transport current as a function of the dimensionless potential difference $\varphi^* = \varphi b / uL$ between the grids for $K^* = 10^{-2}$; 1; 10^6 (curves 1-3), on the assumption that $N = 1$ and $E_0^* = 0$ and 1 (lines with points). It is evident from Fig. 1 that for given φ^* and field at the emitter, K^* in the range 10^{-2} to 10^6 causes less than 10% variation in the transport current, which is due to the ions being absorbed quite weakly by the particles on diffusion-limited electrification. The total transport current (Fig. 1) is a monotonically increasing function of the potential difference.

Figure 2 shows the particle charge at the exit as a function of the transport current for $K^* = 10^6$ and $E_0^* = 0$; 1; 5 (lines 1-3) either neglecting the particle concentration (lines with points) or for $N = 1$. For given transport current and E_0^* , the particle charge increases as the concentration falls, and the larger E_0^* , the less the increase in particle charge. Also, for a given concentration and transport current, the charge decreases as E_0^* increases.

This shows that EHD flow parameters can vary as a result of adding aerosol particles and describes how this occurs; the effects of the particles on the EHD flow increase with the electrification.

2. We consider a one-dimensional stationary flow for a unipolar charged gas between two grounded grids, with the first having a uniform injection of uncharged particles. This is a one-dimensional analog of a uniform charged flow around an aerosol source. The ions may be produced by a corona grid electrode placed upstream in the flow before the first grid.

As in section 1, we take a cartesian coordinate system with the grids in the planes $x = 0$ and $x = L$. As before, the effects from the field and the particle inertia on the motion are taken as small, but the concentration is such that one cannot in general neglect the effects on the field strength and ion space charge.

Any increase in ion concentration in the incident flow (i.e., at $x = 0$) for a given flow speed u means that the transport current j may ultimately attain its maximum possible value, which equals the saturation current [4]. From the physical viewpoint, the limitation on the transport current occurs because an intrinsic electric field arises in the flow, which retards the ions near the $x = 0$ section, which has been examined from theory and experiment in [4] for a pure gas not containing particles, where it was shown theoretically that the dimensionless saturation transport current $j_s^* = 9/8$ (for grounded grids). If there are particles whose mobility is much less than the ionic mobility, the saturation current is increased because the ions deposit on the particles. We further consider how the particles influence the EHD parameters on the basis that the space charge density at the emitter is known. As before, (1.1) and (1.2) describe the distributions for the electrical quantities and the particle charging, but the boundary conditions are

$$x^* = 0, \quad \varphi^* = 0, \quad e_p^* = 0, \quad q^* = \quad x^* = 1, \quad \varphi^* = 0. \quad (2.1)$$

A difference from section 1 is that we examine the more general case where the electrical Peclet number ($Pe_E = Pe|E^*|$, $Pe \equiv au/D$) is not small. As for $Pe_E \geq 1$ one needs to incorporate the effects from the field on the particle charging; to derive I^* in (1.1) we use the solution for the two-dimensional treatment of the ion distribution near an immobile and ideally conducting sphere in an external electric field, which absorbs ions [3]; K^* is taken as infinite.

On these assumptions, the flow is characterized by the three dimensionless parameters q_0^* , N , Pe ; the last here defines the electrification mechanism. For example, for $Pe \rightarrow 0$, we have also $Pe_E \equiv Pe|E^*| \rightarrow 0$, and the particle charging is diffusion-limited, while for $Pe \geq 1$, there is mixed charging from ion diffusion and deposition on the particles due to the field. For $Pe \gg 1$ and $|E^*| \geq 1$, the ion diffusion can be neglected in determining I^* .

The calculations showed that the particles influence the flow considerably for $N \geq 1$, the effect increasing with Pe . However, at large $NI^0 = \Omega$ ($I^0 = I^*(Pe, 0)$), it is difficult to integrate the equations numerically because a small parameter appears before the derivative in one of the equations. The linked asymptotic expansion method [7] enables one to obtain an approximate interior solution for the boundary layer having thickness $\delta = 1/\Omega$ near the emitter and an exterior solution for the region $O(\delta) < x \leq 1$.

From these we get the combined uniformly suitable solution

$$E^* = G \left(1 - \frac{G^2}{2\Omega} \right) \left(x^* - \frac{1}{2} \right) - \frac{G^2}{2\Omega} \exp(-g\Omega x^*) + O\left(\frac{1}{\Omega^2}\right), \quad e_p^* = \frac{G}{N} [1 - \exp(-g\Omega x^*)] + O\left(\frac{1}{N\Omega}\right), \quad (2.2)$$

$$q^* = q_0 \left[1 + O\left(\frac{1}{\Omega}\right) \right] \exp(-g\Omega x^*), \quad j^* = G \left(1 - \frac{G}{2\Omega} \right) + O\left(\frac{1}{\Omega^2}\right),$$

$$g = 1 + \frac{q_0^*}{2}, \quad G = \frac{2q_0^*}{2 + q_0^*}.$$

In deriving (2.2), we have not used any detailed forms for $I^*(Pe_E, e_p^*)$ and $I^0(Pe)$. In particular, on the assumptions made at the start, we have [8, 9]

$$Pe \rightarrow 0: \quad I^0 = 1 + \frac{1}{2} Pe + O(Pe^2), \quad (2.3)$$

$$Pe \rightarrow \infty: \quad I^0 = \frac{3}{4} Pe + \frac{1}{2} + O(Pe^{-1/2}).$$

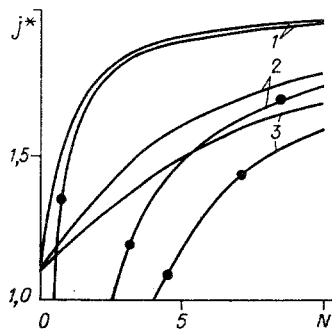


Fig. 5

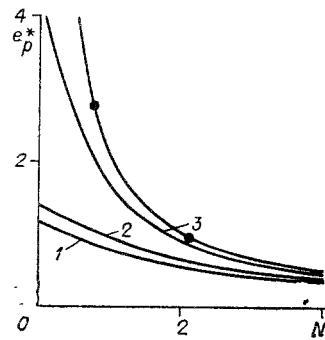


Fig. 6

It follows from (2.2) and (2.3) that for sufficiently large $\Omega = NI^0$ and Pe , the effects from the particles on the flow are determined by NPe .

If q_0^* and Ω increase, the boundary layer near the emitter thins. At saturation ($q_0^* = \infty$), the boundary layer is $\delta \sim \Omega^{-2}$, and instead of (2.2) we have

$$\begin{aligned}
 E^* &= (2x^* - 1) \left(1 - \frac{2}{\Omega}\right) + \frac{2}{\Omega} \left[F\left(\frac{\Omega^2 x^{*2}}{2}\right) - 1 \right] + O\left(\frac{1}{\Omega^2}\right), \\
 e_p^* &= \frac{2}{N} F\left(\frac{\Omega^2 x^{*2}}{2}\right) + O\left(\frac{1}{\Omega N}\right), \\
 q^* &= \Omega \left[\frac{1}{F\left(\frac{\Omega^2 x^{*2}}{2}\right)} - 1 + O\left(\frac{1}{\Omega}\right) \right], \quad j^* = 2 \left(1 - \frac{2}{\Omega}\right) + O\left(\frac{1}{\Omega^2}\right).
 \end{aligned} \tag{2.4}$$

F is defined implicitly by $x = F(x) - \ln[1 - F(x)]$; for large values of the argument, the asymptote is $F(x) = 1 - e^{1-x} + o(e^{-x})$. Formulas (2.4) resemble (2.2) in being uniformly suitable for the range $0 \leq x^* \leq 1$.

It follows from (2.2)-(2.4) that any increase in Pe and N leads to a rapid fall in the particle charges at the exit and in the space charge between the electrodes. The transport current increases and at saturation may be twice that in the absence of the particles, $9u^2/(32\pi bL)$ [4]. These conclusions are confirmed by computer solutions shown in Figs. 3-6.

Figure 3 gives calculations on j^* (solid lines) and e_p^* (dashed lines) as functions of q_0^* for $Pe = 0$ and $N = 0; 1; 10$ (curves 1-3); those quantities almost reach saturation, i.e., become independent of q_0^* already for $q_0^* \sim 10$, and j^* increases with N , while e_p^* decreases.

Figure 4 shows q^* distributions in the gap at saturation, i.e., for $q_0^* = \infty$. As x^* increases, the space charge monotonically decreases, and the Peclet number is taken as one, with lines 1-3 corresponding to $N = 0; 1; 5$. For $N = 0$ (particle concentration negligible) and $N = 1$, the ions lie mainly near the emitter.

At a sufficiently high concentration ($N \geq 5$), the rapid ion uptake by the particles means that q^* is close to zero outside a layer having thickness $\sim \Omega^{-2}$ near the emitter. The particles acquire their main charge for $x^* \leq \Omega^{-2}$.

Figure 5 shows calculations of j^* as a function of N for $q_0^* = \infty$ and various Pe . As $j^*(N)$ is monotone, it and (2.4) imply that the dimensionless electrification current is always in the range $9/8 < j^* < 2$, and Fig. 5 shows that the approach in $j^*(N)$ to the limit $j^* = 2$ as N increases is much more rapid for $Pe = 10$ (line 1) than for $Pe = 1$ and 0 (lines 2 and 3) because of substantially accelerated charge exchange between the phases as Pe increases and the associated increase in the local electrical Peclet number. The lines bearing points in Fig. 5 have been constructed from the asymptotic (2.4) formula for j^* , where we assumed $I^0(1) = 1.58$, $I^0(10) = 8.14$ in accordance with the numerical calculations. The accuracy in approximation from (2.4) increases with Pe .

Figure 6 shows the exit particle charge as a function of dimensionless concentration for $q_0^* = \infty$ and $Pe = 0; 1; 10$ (lines 1-3). The particle charge is very much dependent on Pe

only for small N , and as the latter increases, the differences between the curves become slight, and they rapidly approach the asymptote $e_p^* = 2/N$ indicated by the points in Fig. 6.

As an example we consider the flow of an aerosol between two grounded grids separated by $L = 0.1$ m. The flow speed is 4.5 m/sec and the conditions [4] are $a = 2.2 \cdot 10^{-5}$ m, $n_p = 2 \cdot 10^{-10}$ m $^{-3}$, $D = 10^{-5}$ m 2 /sec, $b = 2 \cdot 10^{-4}$ m 2 (V.sec).

Here $Pe = 10$ and $N = 1, 3$. At saturation, the transport current density is $1.5 \cdot 10^{-5}$ A/m 2 , while the particle charge at the collector is $2 \cdot 10^{-16}$ C. If under otherwise constant conditions the particle concentration is reduced to $n_p = 10^7$ m $^{-3}$, the effects from the particles on the flow become negligible and the transport current density falls to 10^{-5} A/m 2 , while the particle charge rises to $5 \cdot 10^{-16}$ C.

LITERATURE CITED

1. S. Sou, Charged-Suspension Dynamics [Russian translation], Mir, Moscow (1975).
2. G. L. Sedova and L. T. Chernyi, "The electrohydrodynamic equations for weakly ionized aerosols showing dispersed-phase particle charging by diffusion," *Izv. Akad. Nauk SSSR, Mekh. Zhidk. Gaza*, No. 1 (1986).
3. A. V. Filippov, "Aerosol-particle charging in an electric field with allowance for ion diffusion," *Izv. Akad. Nauk SSSR, Mekh. Zhidk. Gaza*, No. 1 (1986).
4. A. B. Vatazhin, V. I. Grabovskii, V. A. Likhter, and V. I. Shul'gin, *Electro-Gas Dynamic Flows* [in Russian], Nauka, Moscow (1983).
5. V. V. Ushakov and G. M. Franchuk, "Aerosol particle charging in a one-dimensional electro-gas dynamic flow," *Magn. Gidrod.*, No. 2 (1973).
6. N. L. Vasil'eva and L. T. Chernyi, "Aerosol particle electrification on motion in a one-dimensional corona discharge," *Zh. Prikl. Mat. Tekh. Fiz.*, No. 4 (1982).
7. A. N. Nayfeh, *Perturbation Methods*, Wiley, New York (1973).
8. J. D. Klett, "Ion transport to cloud droplets by diffusion and conduction and the resulting droplet charge distribution," *J. Atmos. Sci.*, 28, 78 (1971).
9. N. L. Vasil'eva, G. L. Sedova, A. V. Filippov, and L. T. Chernyi, "Electrohydrodynamic flows of weakly ionized aerosols involving dispersed-phase particle charging," in: *Abstracts for the 6th All-Union Congress on Theoretical and Applied Mechanics* [in Russian], Tashkent (1986).

STUDY OF A SHOCK WAVE IN A TUBE PRODUCED BY A SPHERICAL EXPLOSION

É. K. Anderzhanov and B. D. Khristoforov

UDC 533.6.011

Empirical expressions were obtained in [1] for parameters of shock waves produced in tubes by explosion of concentrated explosive charges in air, valid for large distances from the center of the explosion, where the piston action of the products can be neglected and the spherical shock wave transforms to planar. Below we will present results of an experimental study of the explosion near-zone. Numerical solution of such a three-dimensional nonlinear nonsteady-state problem is made difficult by the need to consider the complex pattern of interaction of the direct shock wave and reflections from the tube walls, the hydrodynamic instabilities which then develop on the tube axis, and the real properties of the medium, which consists of air mixed with explosion products due to Rayleigh-Taylor instability.

Metallic tubes with radii $r = 1.5$ and 1.9 cm were used in the experiments, with spherical TEN charges of mass $M = 0.8$ and 2.5 g ($\rho = 1.6$ g/cm 3) being detonated on the tube axis. Initiation was accomplished in the center of the charge, using a small amount of lead azide and electrical explosion of a 0.05-mm thick manganin wire penetrating the charge.

The motion of the shock-wave front was photographed by an SFR-2M camera attached to a shadow device through a rectangular window in the tubes in a photorecorder regime. Shock-wave exit from tubes of various length and the hydrodynamic flow pattern were recorded in

Moscow. Translated from *Zhurnal Prikladnoi Mekhaniki i Tekhnicheskoi Fiziki*, No. 5, pp. 25-27, September-October, 1988. Original article submitted March 16, 1987.